Sterically demanding benzene-1,3,5-tricarboxamides: tuning the mechanisms of supramolecular polymerization and chiral amplification†

Martijn A. J. Veld, Daniël Haveman, Anja R. A. Palmans* and E. W. Meijer*

Received 11th June 2010, Accepted 4th October 2010
DOI: 10.1039/c0sm00516a

Benzene-1,3,5-tricarboxamide (BTA) derivatives with one or three phenylalanine octyl ester (PheOct) moieties were synthesized and their supramolecular polymerization and chiral amplification behavior were investigated in mixing experiments between enantiomer pairs and in mixing with another, achiral BTA component. The incorporation of PheOct moieties is shown to have a major impact on the supramolecular self-assembly.

Introduction

Benzene-1,3,5-tricarboxamide (BTA) based monomers (Fig. 1) represent an appealing class of supramolecular polymers with potential applications in nucleating agents for isotactic polypropylene,[1] non-covalent crosslinkers in thermoplastic elastomers,[2] nanostructured materials[3] and organogelators.[4,5] The self-assembly of these disc-shaped molecules results in columnar structures as a result of strong, threefold intermolecular hydrogen bonding and π–π interactions between consecutive monomers.[6] Moreover, both C_3-symmetric BTAs and desymmetrized BTAs with at least two different peripheral substituents are synthetically well accessible *via* amide coupling reactions of activated carboxylic acids with amine nucleophiles, giving access to a wide variety of structurally diverse supramolecular building blocks.[2,7]

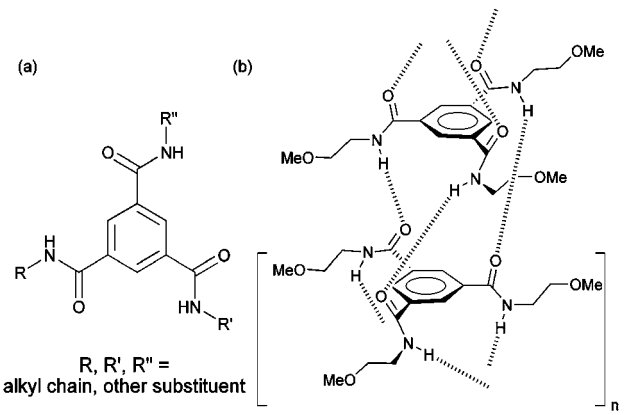

Fig. 1 (a) Common molecular structure of benzene-1,3,5-tricarboxamides (BTAs) and (b) threefold intermolecular hydrogen bonding array as observed in a BTA crystal structure.[6]

Laboratory for Macromolecular and Organic Chemistry, Department of Chemical Engineering and Chemistry, Eindhoven University of Technology, P.O. Box 513, 5600 MB Eindhoven, The Netherlands. E-mail: A.Palmans@tue.nl; E.W.Meijer@tue.nl; Fax: +31 40 245 1036; Tel: +31 40 247 3101

† Electronic supplementary information (ESI) available: Details containing the synthetic procedures for the preparation of compound **1**, additional CD and UV-vis spectra and information on the data fitting procedures are available. See DOI: 10.1039/c0sm00516a

Because of the intrinsic helical nature of the hydrogen bond motif in the supramolecular polymer, a preferred helicity of the aggregates is readily observed by circular dichroism (CD) spectroscopy when one or more stereocenters are present in the substituents of non-racemic BTAs.[8–10] Mechanistically, two types of supramolecular polymerization processes can be distinguished for the self-assembly of these supramolecular motifs.[11] In the first case of isodesmic self-assembly behavior, the association constants for the first and subsequent association steps are equal to one another. As a result, the fraction of aggregated monomer displays a sigmoidal dependence on temperature. In the second situation, the association constants for the first few monomer additions are less favorable than all subsequent monomer additions. This type of behavior is known as the nucleation/elongation or cooperative self-assembly mechanism and is characterized by a sudden change in the fraction of aggregated monomer as a function of temperature or concentration. In BTA derivatives, both types of supramolecular polymerization have been described depending on the molecular structure. The *N*,*N*′,*N*″-tris(alkyl) substitution pattern, for example, results in a highly cooperative self-assembly process,[12–14] whereas bipyridine or dipeptide based substituents give rise to an isodesmic self-assembly behavior.[15,16] The exact reason for the observed differences in the self-assembly process depending on the nature of the side chains has not been fully elucidated, although the ability to form strongly polarised intermolecular hydrogen bonds in the aggregates appears to play an important role in the cooperative self-assembly behavior.[17]

The self-assembly behavior of BTAs can be fine-tuned by adjusting the BTA periphery. The introduction of additional π–π or hydrogen bonding interactions might result in an increased strength of the intermolecular interactions, whereas sterically demanding substituents will weaken these interactions. The large structural diversity and common availability of amino acids make those molecular fragments interesting candidates for systematic studies on the relation between molecular structure and BTA self-assembly behavior. The carboxylic acid group of the amino acid is easily modified, and often both enantiomers of the amino acids are commercially available, allowing for the facile preparation of BTA enantiomer pairs and subsequent chiral amplification studies. BTAs with amino acid derived substituents have been described previously. At high concentrations the formation of long, helical aggregates was shown by

transmission electron microscopy (TEM) studies for BTAs with leucine methyl ester and valine methyl ester derived substituents.[18] Additionally, the possibility to induce a preferential helicity in aggregates of achiral BTAs by the introduction of chiral BTA dopants was shown.[18] More recently, a series of glycine octyl ester (GlyOct), leucine octyl ester (LeuOct) and phenylalanine octyl ester (PheOct) based C_3-symmetric BTAs were prepared and investigated as potential organo-gelators.[19] At high concentrations, the $(PheOct)_3$ BTAs showed the most promising organogelation behavior, suggesting that large, interacting aggregates can be formed. However, detailed studies on the aggregation and chiral amplification behavior in dilute solution were not reported.

In this paper, we report on our ongoing efforts to link the molecular structure of BTAs to the nature of their self-assembly mechanism and their effectiveness in the supramolecular amplification of chirality. We here evaluate the impact of one or three phenylalanine octyl ester (PheOct) moieties on BTA self-assembly behavior in dilute solution. We focused on this moiety as the newly introduced phenyl ring might result in additional and favorable π–π interactions, which are counterbalanced by the increased steric demands. Additionally, the influence of the PheOct moiety on the chiral amplification behavior is studied by means of "majority rules" experiments.[20,21] Finally, we mix the newly synthesized compounds with *N*,*N*′,*N*″-tris(alkyl) BTAs to evaluate their compatibility and to study how the BTA self-assembly process in these mixtures is affected by the presence of the (PheOct) BTAs.

Results and discussion

Synthesis

The synthetic route to PheOct substituted benzene-1,3,5-tricarboxamides is depicted in Scheme 1. Both enantiomers of the target BTAs were prepared to allow a detailed study of the self-assembly and chiral amplification behavior. The synthesis of the four target compounds starts with the esterification of optically pure (*R*)- or (*S*)-phenylalanine with 1-octanol according to a literature procedure.[19] The optically pure phenylalanine octyl esters are subsequently reacted with either freshly prepared bis(octylaminocarbonyl)benzoyl chloride (**1**)[2] or with commercially available benzene-1,3,5-tricarbonyl trichloride to give target BTAs **2** and **4**, respectively. All compounds were purified by column chromatography and were obtained as white solids in excellent purity according to ^{1}H-NMR and elemental analysis.

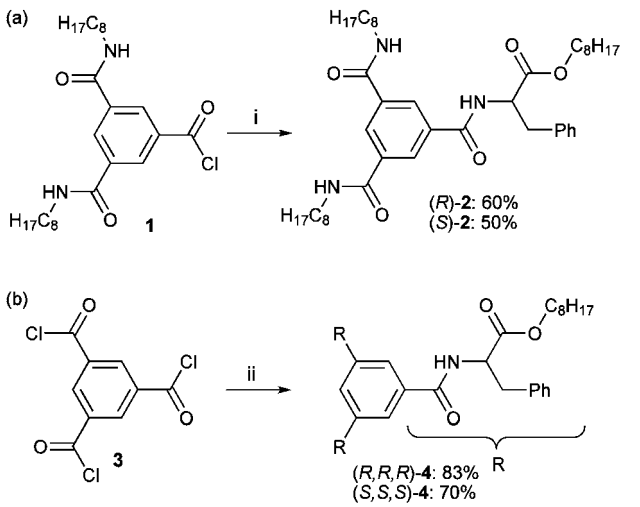

Scheme 1 Synthesis of $(PheOct)$ $(octyl)_2$ BTA (**2**) and $(PheOct)_3$ BTA (**4**). (i) 2 mol eq. (*R*)- or (*S*)-phenylalanine octyl ester, 3 eq. Et_3N, DCM, overnight, rt; (ii) 3.2 mol eq. (*R*)- or (*S*)-phenylalanine octyl ester, 3.5 mol eq. Et_3N, DCM, 3 h, 0 °C to rt.

Self-assembly mechanism of PheOct derived BTAs

Whereas the self-assembly of *N*,*N*′,*N*″-tris(alkyl) BTAs is strongly cooperative,[14] the impact of bulky amino acid groups on the mechanism of self-assembly in BTAs is not trivial to predict. We studied the self-assembly mechanism of the PheOct BTA derivatives by means of UV-vis and CD spectroscopy in dilute solution. The spectral data of the PheOct BTA derivatives were measured in methylcyclohexane (MCH), a solvent in which BTAs aggregate, and in acetonitrile (MeCN), in which BTAs are molecularly dissolved.[14]

The CD effect of ((*S*)-PheOct) $(octyl)_2$ BTA ((*S*)-**2**) at a concentration of 4.6×10^{-5} M in MCH consists of a single, positive band in the wavelength region between 205 and 275 nm (Fig. 2a, solid black line). The CD spectrum closely resembles the spectrum of a chiral *N*,*N*′,*N*″-tris(alkyl) BTA, indicating a helical organization of the benzene-1,3,5-tricarboxamide chromophore.[14] Moreover, the size of the CD effect ($\Delta\varepsilon = 30$ L mol^{-1} cm^{-1} at 220 nm, $g = 1.7 \times 10^{-3}$) is similar to the value observed for chiral, *N*,*N*′,*N*″-tris(alkyl) substituted BTAs ($\Delta\varepsilon = 40$ L mol^{-1} cm^{-1} at

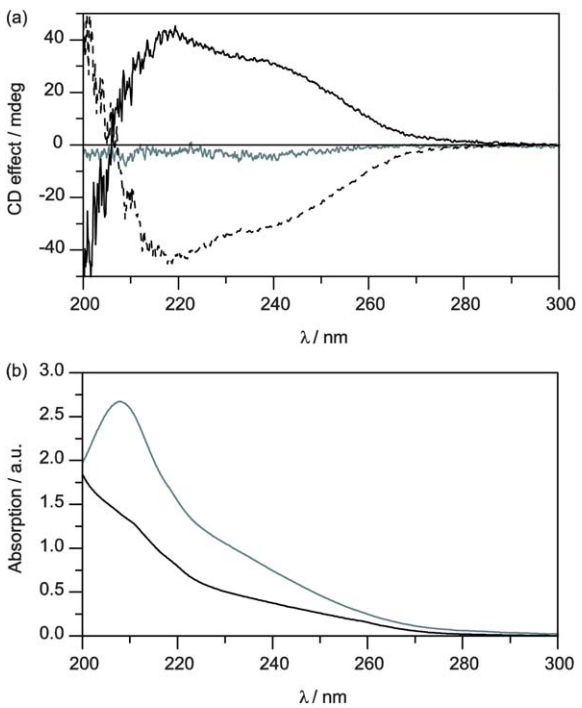

Fig. 2 (a) CD spectra for $(PheOct)$ $(octyl)_2$ BTAs (*S*)-**2** (solid black line) and (*R*)-**2** (dashed black line). The molecularly dissolved state of (*S*)-**2** in MeCN is shown as well (solid gray line). (b) UV-vis spectra for (*S*)-**2** in MCH (black line) and MeCN (gray line) (all measurements: $c = 4.6 \times 10^{-5}$ M).

220 nm, $g = 1.6 \times 10^{-3}$).[13] As expected, a perfect mirror-image CD spectrum was found for (*R*)-**2** (Fig. 2a, dashed black line), whereas the molecularly dissolved state of (*S*)-**2** in MeCN displays a weakly negative CD effect of 3 mdeg at $\lambda = 225$ nm (Fig. 2a, gray line). This small, residual CD effect most likely originates from the chiral arrangement around the phenyl group of the amino acid. The UV-vis spectrum of the aggregated state is blue shifted compared to the molecularly dissolved state (Fig. 1b, black and gray line, respectively), indicative of H-type aggregates.[22]

Solutions of BTAs (*S*,*S*,*S*)-**4** and (*R*,*R*,*R*)-**4** in MCH display mirror-shaped CD spectra as expected for a pair of enantiomers (Fig. 3a, solid and dashed black lines, respectively). Interestingly, the CD spectrum of BTA **4** shows a bisignate Cotton effect (Fig. 3a) in the wavelength region between 200 nm and 270 nm and its shape is completely different from that of mono-PheOct BTA **2** (overlay shown in Fig. S1†). In addition, the value of $\Delta\varepsilon$ at $\lambda = 225$ nm (76 L mol^{-1} cm^{-1}; $g = 2.8 \times 10^{-3}$) is around 2.5 times higher than that of BTA **2**. No significant CD effect is present for the molecularly dissolved state in MeCN (Fig. 3a, gray line). The UV-vis spectra of the aggregated state in MCH and the molecularly dissolved state in MeCN at a concentration of 1×10^{-5} M are very similar (Fig. 3a, black and gray line, respectively).

Temperature dependent UV-Vis and CD measurements provide detailed information about the mechanism of supramolecular aggregation.[23] The changes in intensity of the CD effect and UV-vis absorption at $\lambda = 225$ nm were monitored while cooling a solution of BTA (*S*)-**2** in MCH from 90 °C to 20 °C at a rate of 2 °C min^{-1} (full spectra in Fig. S2†). Both the UV-vis and CD data showed a sigmoidal dependence of the spectral data with temperature after normalization of the data (Fig. 4), which is indicative of an isodesmic type of self-assembly behavior.

The temperature-dependent cooling curves of (*S*)-**2** were fitted using an isodesmic self-assembly model to quantify the data (details in ESI†) and three important parameters, T_m, the temperature at which half of the monomer is aggregated, ΔH_e, the enthalpy of elongation and, the association constant K at a certain temperature were extracted from the data (Table 1). The T_m and ΔH values obtained from simultaneous UV-vis and CD measurements are in good correspondence with one another.

The small differences in thermodynamic parameters as determined by these two techniques are most likely the result of additional changes in the shape of the UV-vis spectra with temperature, whereas in the CD spectra only the signal intensity changes.

For BTA **4**, the differences in the UV-vis spectra as a function of temperature were too small to assess the degree of aggregation as a function of temperature. Therefore, we monitored the intensity of the CD effect at $\lambda = 225$ and 245 nm to obtain temperature dependent spectral data. No evidence for a cooperative aggregation process was observed for solutions of BTA (*S*,*S*,*S*)-**4** in MCH at concentrations between $c = 5 \times 10^{-6}$ and 5×10^{-5} M. Instead, the temperature dependent CD measurements showed a nearly linear variation of the signal intensity with temperature (Fig. 4b and S3†). Interestingly, BTA **4** cannot be fully aggregated or molecularly dissolved between 20 and 90 °C, making it impossible to determine the mechanism of the self-assembly process from the temperature dependent cooling curve. The changes in the shape of the CD spectra upon

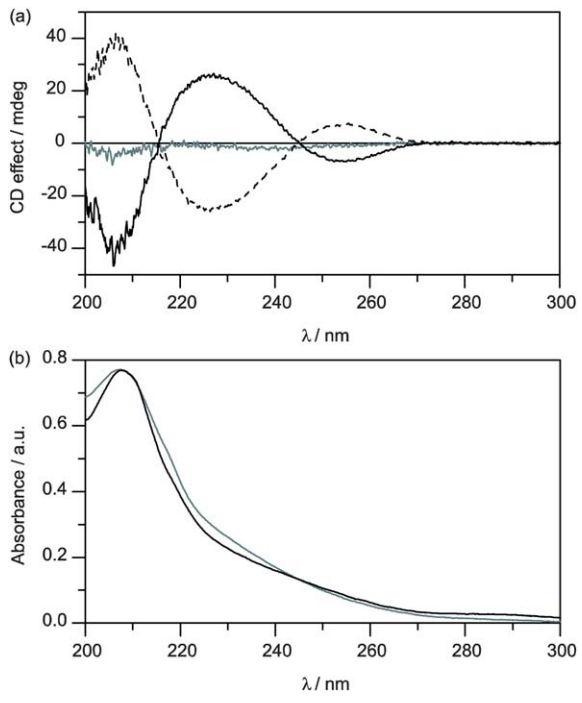

Fig. 3 (a) CD spectra in MCH for (*S*,*S*,*S*)-**4** (solid black line) and (*R*,*R*,*R*)-**4** (dashed black line). The molecularly dissolved state of (*S*,*S*,*S*)-**4** in MeCN is also shown (solid gray line). (b) UV-vis spectra for (*S*,*S*,*S*)-**4** in MCH (black line) and MeCN (gray line) (all measurements: $c = 1 \times 10^{-5}$ M, 20 °C).

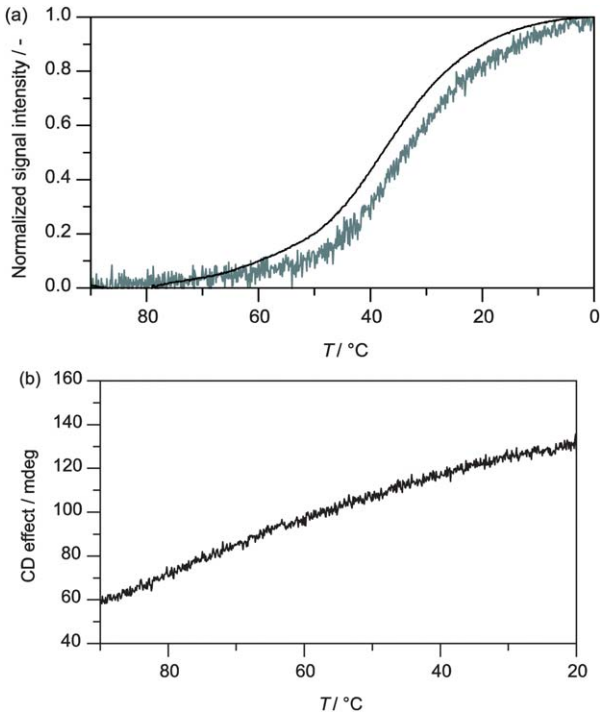

Fig. 4 (a) Normalized data for cooling curves of (*S*)-**2** as determined by UV-vis (black line) and CD spectroscopy (gray line) ($c = 4.6 \times 10^{-5}$ M, MCH) and (b) temperature dependence of the CD effect of (*S*,*S*,*S*)-**4** ($c = 5.0 \times 10^{-5}$ M, MCH).

Table 1 Thermodynamic parameters characterizing the isodesmic self-assembly behavior of BTA (*S*)-**2** according to CD and UV-vis spectroscopy ($c = 4.6 \times 10^{-5}$ M, MCH)

Method	T_m/K	ΔH_e/kJ mol^{-1}	K (25 °C)/M^{-1}
UV-vis	310.6	-98.8 ± 0.4	$11.4 \pm 0.16 \times 10^4$
CD	306.5	-107.4 ± 1.1	$8.2 \pm 0.25 \times 10^4$

increasing the temperature (Fig. S3†) suggest that ill-defined aggregates are formed.

While the self-assembly of *N*,*N*′,*N*″-tris(alkyl) BTAs was previously found to be strongly cooperative, the presence of one PheOct moiety suffices to change the self-assembly mechanism into an isodesmic behavior in (*S*)-**2**. The introduction of one sterically demanding group clearly has a dramatic influence on the nature of the self-assembly process. In other words, the nucleation step as observed for tris(alkyl) BTAs, which is the result of the formation of a macrodipole upon aggregation,[17] is possibly hampered by introduction of the PheOct moiety. Most likely, the large steric demands of the PheOct moiety play an important role, but the introduction of additional π–π interactions and hydrogen bonding to the ester group may also have an influence.[19] The largely increased steric demands by introduction of the PheOct moiety are immediately visible from the molecular structure (Fig. 5). A direct result of the isodesmic aggregation behavior is that only relatively small aggregates are present for the PheOct derived BTAs in apolar organic solvents at concentrations of typically 5×10^{-5} M ($DP_N = 2.9$), whereas (octyl)$_3$ BTA forms long, helical aggregates under otherwise identical conditions ($DP_N \geq 1000$).[14]

Amplification of chirality in PheOct derived BTAs

In aggregates of chiral, tris(alkyl) substituted BTAs, a small enantiomeric excess (ee) is sufficient to induce a preferred helicity when enantiomers are mixed.[24,25] This effect is known as the "majority rules" effect. The chiral nature of the PheOct moiety and the formation of homochiral aggregates by optically pure BTAs **2** and **4** triggered us to investigate the chiral amplification behavior of these BTAs.

CD spectra of solutions of BTA **2** with varying ee values (full spectra in Fig. S4a†) were measured at a total concentration of 5×10^{-5} M in MCH and the CD effect at $\lambda = 225$ nm was plotted as a function of the ee (Fig. 8, black squares). Although the net helicity ($\Delta\varepsilon/\Delta\varepsilon_{max}$) shows a clear deviation from linearity (Fig. 6, straight line), the majority rules effect is rather weak. Nevertheless, these results show that enantiomers of **2** can be incorporated into aggregates of their non-preferred helicity. As a result of the isodesmic self-assembly behavior of BTA **2**, only small aggregates are present at $c = 5 \times 10^{-5}$ M ($DP_N = 2.9$) prohibiting quantification of the MR effect under these conditions.[26] In contrast, the sterically more demanding BTA **4** did not show a majority rules effect (Fig. 6, white circles, full spectra in Fig. S4b†).[27]

For chiral tris(alkyl) substituted BTAs possessing methyl groups at the chiral centre, strong majority rules effects are generally found *i.e.* a large amount of monomers can be incorporated into aggregates of non-preferred helical sense. Upon introduction of a PheOct substituent into a BTA, the ability to incorporate monomers into an aggregate of non-preferred helical sense is strongly reduced. For BTA **2**, limited amounts of monomers can be incorporated into aggregates of the wrong helicity as shown by the small majority rules effect. The low amount of chiral amplification is directly related to the isodesmic self-assembly process of compound **2**, which, on average, results in relatively small aggregates under the given experimental conditions.[21] (PheOct)$_3$ BTA **4** completely lacked a majority rules effect, suggesting either a zero or very high energetic penalty for incorporation of the non-preferred enantiomer in a chiral

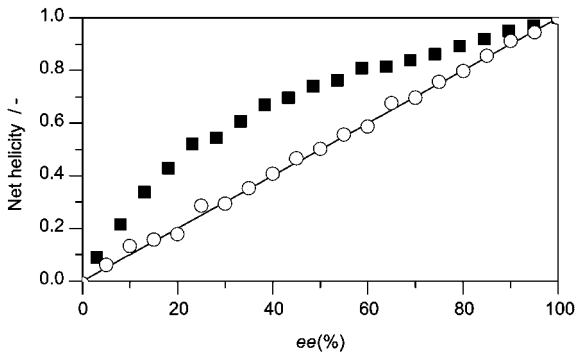

Fig. 6 $\Delta\varepsilon$ at $\lambda = 225$ nm as a function of ee as determined for BTA **2** (■, $c = 5 \times 10^{-5}$ M) and **4** (○, $c = 1 \times 10^{-5}$ M). The solid lines represent a situation without any amplification of chirality (all data: MCH, 20 °C).

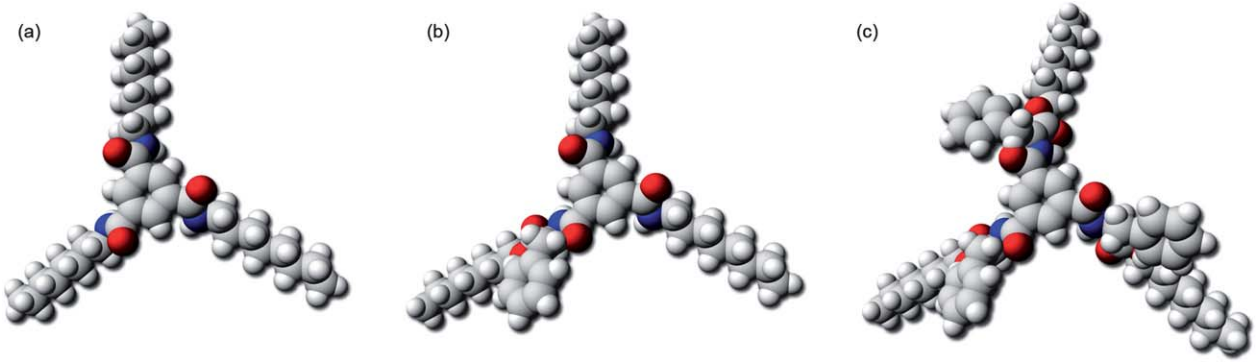

Fig. 5 3D-space filling models showing the increasing steric demands by introduction of the PheOct moiety: (a) (octyl)$_3$ BTA; (b) (PheOct) (octyl)$_2$ BTA (**2**) and (c) (PheOct)$_3$ BTA (**4**).

aggregate. The sterically demanding structure of BTA **4** (Fig. 5c) hints towards the latter possibility and as a result separate aggregates with opposite helicity are formed for both BTA enantiomers. Therefore, the formation of aggregates with opposite helicity for the two BTA enantiomers is a likely explanation for the linear relationship between the ee and observed CD effect.

Mixed aggregates of PheOct derived BTAs and (octyl)$_3$ BTA

Both PheOct substituted BTAs and (octyl)$_3$ BTAs form columnar aggregates in dilute MCH solutions with the difference that self-assembly in PheOct substituted BTAs is isodesmic while in (octyl)$_3$ BTAs self-assembly occurs in a cooperative way. Therefore, it is interesting to investigate whether PheOct substituted BTAs and (octyl)$_3$ BTAs form mixed aggregates and if so, which type of self-assembly behavior will dominate in the mixed aggregates.

Mixtures of chiral BTA (*S*)-**2** with achiral (octyl)$_3$ BTA in MCH were studied first. The $\Delta\varepsilon$ of samples of varying composition was measured at $\lambda = 225$ nm at a total BTA concentration of 5×10^{-5} M (Fig. 7a, full spectra in Fig. S5†). A remarkable and very steep increase in the magnitude of the CD effect was observed upon addition of the initial 5 mol% of (*S*)-**2**, while the $\Delta\varepsilon$ values leveled off after 10 mol% (*S*)-**2** and finally reached the value observed for pure (*S*)-**2**. BTA (*S*)-**2** is thus able to induce a preferential helicity in aggregates mainly consisting of (octyl)$_3$ BTA, showing that the chirality present in (*S*)-**2** can be efficiently transferred. Maximum amplification of chirality was observed at a fraction of chiral BTA as low as 5 mol%.

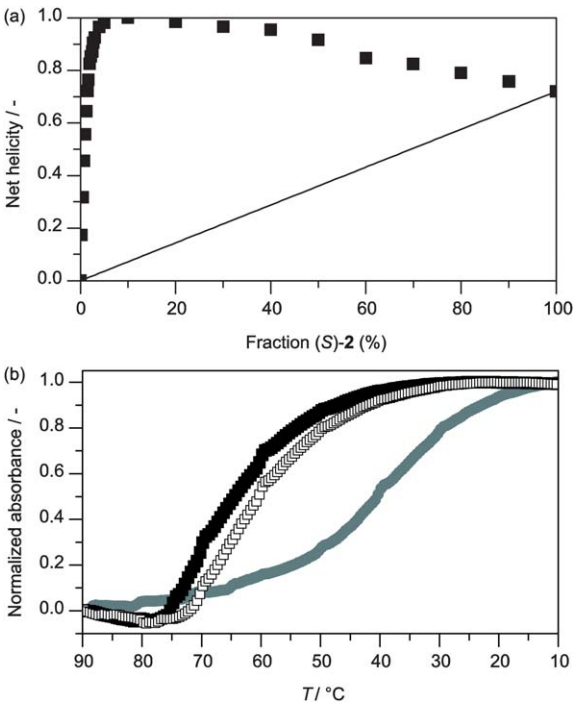

Fig. 7 (a) Mixing experiment of (*S*)-**2** and (octyl)$_3$ BTA showing a maximum CD effect at $x_{(S)\text{-}2} = 0.05$. The data are normalized to the maximum CD effect at $\lambda = 225$ nm, $c_{total} = 5 \times 10^{-5}$ M, MCH, 20 °C. The solid line represents the situation where only dilution effects are operative. (b) Normalized temperature-dependent UV-vis absorbance of (octyl)$_3$ BTA (filled black squares), a mixture of (octyl)$_3$ BTA and (*S*)-**2** (open squares; $x_{(S)\text{-}2} = 0.20$), and (*S*)-**2** BTA (filled grey squares) (λ = 225 nm, data normalized to absorbance values at 90 °C and 10 °C).

We expect that the average size of the mixed aggregates strongly depends on the composition of the sample due to the different supramolecular self-assembly mechanisms of (octyl)$_3$ BTA (cooperative) and **2** (isodesmic). To study this transition from a highly cooperative to an isodesmic type of self-assembly behavior in more detail, temperature dependent UV-vis measurements were performed on a sample with $x_{(S)\text{-}2} = 20$ mol% (Fig. 7b and full spectra in Fig. S6†) and compared to those of pure (octyl)$_3$ BTA and pure (*S*)-**2**. Since (octyl)$_3$ BTA is achiral, only UV temperature dependent measurements allow for comparison between the three samples. A similar UV cooling curve was obtained for the sample with 20 mol% (*S*)-**2** and for a sample containing pure (octyl)$_3$ BTA. In both cases cooperative self-assembly behavior is present (Fig. 7b) as can be seen from a sudden change in the degree of aggregation with a decrease in temperature. The thermodynamic parameters (T_e, h_e, and K_a) that describe the cooperative self-assembly process (Table 2) were extracted from the data.[14] These parameters are the temperature of elongation (T_e) at which the self-assembly process starts, the enthalpy gain upon aggregation after the nucleation step (h_e) and the association constant of the nucleation step (K_a). The latter parameter is a measure for the degree of cooperativity shown by the supramolecular system and the smaller its value is, the more cooperative the aggregation process.

Comparing the thermodynamic parameters for the sample $x_{(S)\text{-}2} = 0.20$ and pure (octyl)$_3$ BTA shows only minor differences. The higher temperature at which the self-assembly process starts in the pure (octyl)$_3$ sample (Table 2, entry 1) can be explained by the 20% lower (octyl)$_3$ concentration in the mixed sample. Secondly, the enthalpy of elongation (h_e) shows a more negative value for pure (octyl)$_3$ BTA than for the mixed aggregates. This means that the formation of mixed aggregates is energetically a slightly less favorable from an enthalpic point of view. Third of all, the difference in nucleation constant (K_a) between the two measurements is relatively small, showing that the nucleation step is not strongly affected by the presence of (*S*)-**2**. Apparently, the incorporation of (*S*)-**2** into mixed aggregates is the energetically most favorable situation, although a small enthalpic penalty needs to be paid by the formation of less-stable aggregates.

The sterically demanding PheOctyl moiety present in BTA (*S*)-**2** effectively induces a preferential helicity in mixed aggregates with (octyl)$_3$ BTA. To see whether a further enhancement is possible by introduction of three PheOct moieties, mixing experiments between (*S*,*S*,*S*)-**4** and (octyl)$_3$ BTA were performed at a total concentration of 1×10^{-5} M. Full CD spectra of various compositions were measured directly after mixing of the two components.[29] A clear interaction between the two BTAs was observed although no amplification of chirality was found

Table 2 Thermodynamic parameters for the self-assembly process of pure (octyl)$_3$ BTA and a mixture with 20 mol% (*S*)-**2** ($\lambda = 225$ nm, $c_{total} = 5 \times 10^{-5}$ M, MCH)

Entry	$x_{(S)\text{-}2}$ (mol%)	T_e/K	h_e/kJ mol^{-1}	K_a (—)
1	0	347.9	-71.6 ± 0.3	1.9×10^{-4}
2	20	344.1	-64.6 ± 0.3	5.4×10^{-4}

(Fig. 8a). Surprisingly, two different regimes are observed, depending on which of the two BTAs is present in excess (Fig. 8c).

The regime in which $(octyl)_3$ BTA is in excess ($0 \leq x_{(S,S,S)\text{-}4} < 0.50$) shows a linear relationship between the amount of (*S*,*S*,*S*)-**4** and the intensity of the CD spectrum, while the shape of the CD spectrum is independent on the composition (full spectra in Fig. S7a†). Interestingly, the shape and magnitude of the CD spectrum with $x_{(S,S,S)\text{-}4} = 0.50$ (Fig. 8b, black line) are different from that of a sample of pure (*S*,*S*,*S*)-**4** at half of the original concentration (Fig. 8b, gray line). In the mixed sample two additional bands are observed around $\lambda = 245$ nm and 260 nm (Fig. 8b, black line), showing that this spectrum must be attributed to a different species than an aggregate of pure (*S*,*S*,*S*)-**4**. This gradual change suggests the formation of a heterocomplex with 1 : 1 stoichiometry between BTAs (*S*,*S*,*S*)-**4** and $(octyl)_3$ BTA until all $(PheOct)_3$ BTA has been consumed.

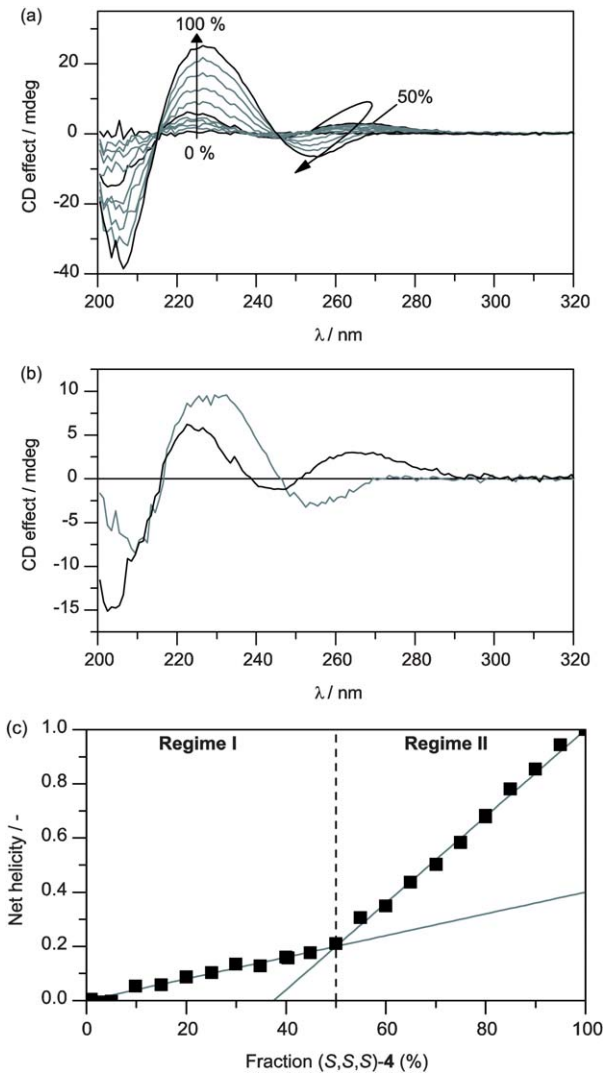

Fig. 8 (a) Full CD spectra at 10 mol% increments for a mixing experiment between (*S*,*S*,*S*)-**4** and $(octyl)_3$ BTA ($c_{total} = 1 \times 10^{-5}$ M, MCH, 20 °C). The solid black line in the middle shows the sample containing 50% (*S*,*S*,*S*)-**4**. (b) Comparison of CD spectra of a mixture of (*S*,*S*,*S*)-**4** and (octyl)3 BTA ($x_{(S,S,S)\text{-}4} = 0.50$) at $c_{total} = 1 \times 10^{-5}$ M (black line) and a solution of pure (*S*,*S*,*S*)-**4** at $c = 5 \times 10^{-6}$ M (gray line). (c) Mixing experiment between (*S*,*S*,*S*)-**4** and $(octyl)_3$ BTA showing the existence of two different regimes depending on the BTA present in excess (data shown for: $\lambda = 225$ nm, $c_{total} = 1 \times 10^{-5}$ M, MCH, 20 °C).[28]

The second part of the titration curve with excess (*S*,*S*,*S*)-**4** ($0.5 < x_{(S,S,S)\text{-}4} \leq 1.0$) displays a gradual change of the CD spectrum from the 1 : 1 complex into that of pure (*S*,*S*,*S*)-**4** (full spectra in Fig. S7b†). The numerically average of the spectra from the 1 : 1 complex and a solution of pure (*S*,*S*,*S*)-**4** was identical to the experimentally determined spectrum of a sample with 75 mol% (*S*,*S*,*S*)-**4**. This suggests that for all compositions in this range, the 1 : 1 complex is formed until all $(octyl)_3$ BTA has been consumed, while the excess (*S*,*S*,*S*)-**4** is present in separate aggregates.

To substantiate the formation of a stable heterocomplex with 1 : 1 stoichiometry between (*S*,*S*,*S*)-**4** and $(octyl)_3$ BTA further, temperature dependent measurements were performed for solutions containing 25, 50 and 75 mol% of (*S*,*S*,*S*)-**4** and a total concentration of 1×10^{-5} M (cooling curves and full spectra in Fig. S8†). Interestingly, the UV cooling curves of solutions containing 0 or 25 mol% chiral BTA **4** are similar and show a cooperative self-assembly behavior. The sample containing 25 mol% (*S*,*S*,*S*)-**4** displayed changes in the UV spectra similar to those observed for a pure $(octyl)_3$ BTA solution at $c = 5 \times 10^{-6}$ M. The shape of the cooling curve for this sample and the temperature of elongation ($T_e = 316$ K) were nearly identical to the results found for a 5×10^{-6} M solution of pure $(octyl)_3$ BTA ($T_e = 317$ K). These observations are indicative for the independent formation of separate aggregates of $(octyl)_3$ BTA. In contrast, the UV cooling curve of solutions containing 50 or 75 mol% chiral BTA **4** is similar to that of pure (*S*,*S*,*S*)-**4** and clearly shows an isodesmic behavior. These observations are a strong indication towards the preferential formation of a heterocomplex with 1 : 1 stoichiometry next to aggregates of the BTA that are present in excess, as is schematically shown in Fig. 9.[30]

Conclusions

The introduction of a phenylalanine octyl ester (PheOct) moiety in BTAs has a distinct influence on the supramolecular self-assembly behavior. In contrast to tris(alkyl) substituted BTAs no cooperative type of self-assembly behavior is observed and an isodesmic self-assembly mechanism is found instead. As a result, this class of compounds is less suitable for application as low molecular weight organogelators, since relatively high concentrations are required to reach sufficiently large, interacting aggregates that finally result in the gel state. The influence of the steric demands of the PheOct moiety becomes clearly visible in mixing experiments with achiral *N*,*N*′,*N*″-tris(octyl) BTA and in mixing experiments between the PheOct BTA enantiomers. The mixing experiments with $(octyl)_3$ BTA reveal a strong interaction between both PheOct BTAs and the tris(alkyl) achiral BTA. For BTA **2** a strong amplification of chirality was observed, whereas $(PheOct)_3$ BTA **4** showed the preferential formation of a 1 : 1 heterocomplex with $(octyl)_3$ BTA, without the induction of a preferred helicity in aggregates consisting of mainly $(octyl)_3$ BTA. A weak majority rules effect is observed for **2**, which is the result of the relatively small average aggregate size due to the isodesmic self-assembly process. Therefore only limited amounts of monomers can be incorporated into aggregates of non-preferred helicity. Moreover, the increased steric requirements for the PheOct moiety might further limit the incorporation of

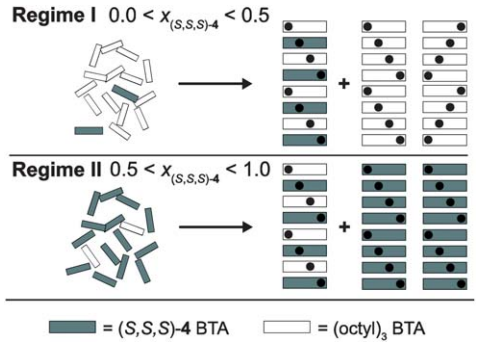

Fig. 9 Schematic representation of the mixing experiments with (*S*,*S*,*S*)-**4** and (octyl)$_3$ BTA showing the preferential formation of a 1 : 1 heterocomplex and separate aggregates for the BTA present in excess. (The cartoon only indicates the formation of mixed aggregates and does not state anything about the relative size of the various aggregates).

monomers with a non-preferred configuration at the stereocentre. The latter effect was even more pronounced for BTA **4**, which did not show a majority rules effect at all. The self-assembly and chiral amplification studies on the PheOct derived BTAs show a highly interesting and sometimes surprising self-assembly behavior. Clearly, the class of amino acid ester substituted BTAs is attractive enough to be examined in more detail in the future to get a better insight into the supramolecular behavior of these BTA aggregates.

Experimental section

Materials and equipment

Detailed information on the origin of the used chemicals and used equipment for analysis of the synthesized compounds can be found in the ESI†. UV-vis and CD measurements were performed on a Jasco J-815 spectropolarimeter using spectrograde MCH as solvent. The sensitivity, time constant and scan rate were chosen appropriately. Temperature-dependent measurements were performed with a PFD-425S/15 Peltier-type temperature controller and an adjustable temperature slope. Unless stated otherwise, a temperature gradient of 2 °C min^{-1} was used. In all other measurements, the temperature was set at 20 °C.

Procedure for UV-vis and CD measurements

The desired amount of compound was weighed out and dissolved in the appropriate amount of solvent to directly reach the desired concentration, unless otherwise stated. The solutions were carefully heated, allowed to cool to rt and sonicated for at least 10 min, heated again and cooled to rt. The heating and sonication procedure was performed each time an earlier prepared solution was used. In the mixing experiments, at least 2500 μL of solution containing the first component were put into a 1 cm cuvette. Appropriate amounts of solutions with the second component were added using a microlitre syringe, after which the cuvette was closed and mixed well by shaking. The sample was put back into the spectrometer which was kept at the desired temperature (20 °C) and equilibrated for at least 1 min, after which the spectrum was recorded.

Synthetic procedures

The preparation of monoacid chloride **1** according to a modified literature procedure[2] is described in the ESI†. Both enantiomers of optically pure phenylalanine octyl ester were synthesized according to a literature procedure.[19] Since phenylalanine octyl ester turned out to be unstable upon storage, a double amount of this partially degraded compound was used in the amide coupling for the syntheses of **2** and **4**.

***N′*,*N″*-Dioctyl-*N*-[(*S*)-(benzyl)octyloxycarbonylmethyl]benzene-1,3,5-tricarboxamide ((*S*)-2).** Under an argon atmosphere, a solution of 3,5-bis(*N*-octylaminocarbonyl)benzoyl chloride (**1**) (170 mg, 0.31 mmol) in dry DCM (2 mL) was prepared. A solution of L-phenylalanine octyl ester (182 mg, 0.65 mmol, 2.1 eq.) and Et_3N (140 μL, 1.0 mmol, 3.3 eq.) in dry DCM (4 mL) was added by syringe over a 10 min interval while stirring at rt. Stirring was continued overnight, after which the reaction mixture was diluted with DCM (10 mL) and washed with 1 M HCl (2 × 15 mL). During extraction, 2-propanol (4 mL) was added to improve phase separation. The organic layer was dried over Na_2SO_4, filtered and concentrated *in vacuo* to give the crude product, which was purified by manual column chromatography over normal silica gel (heptane/EtOAc 2 : 1, R_f = 0.15). BTA (*S*)-**2** was isolated as a sticky white solid (108 mg, 0.15 mmol, 50%). ^{1}H-NMR ($CDCl_3$): 8.24 (s, 1H, ArH (core)), 8.16 (s, 2H, –ArH (core)), 7.34–7.18 (m, 5H, –Ph (Phe)), 7.16 (d, 1H, J = 7.7 Hz, –CONH–(Phe)), 6.55 (t, 2H, J = 5.3 Hz, –CONH–(octyl)), 5.02 (ddd, 1H, J = 7.7, 6.7, 6.0 Hz, –CONHC*H*RR′–), 4.16–4.10 (m, 2H, –$COOCH_2$–), 3.44 (dt, 4H, J = 5.3, 5.2 Hz, –CONHCH_2–), 3.28 (dd, 1H, J = 13.7, 6.0 Hz, Hα–CH_2Ph), 3.22 (dd, 1H, J = 13.7, 6.7 Hz, Hβ–CH_2Ph), 1.71–1.53 (m, 6H, –$COOCH_2CH_2$– + –$CONHCH_2CH_2$–), 1.44–1.19 (m, 30H, –CH_2–), 0.88 (t, 9H, J = 5.5 Hz, –CH_3) ppm. ^{13}C-NMR ($CDCl_3$) δ: 171.7, 165.7, 165.5, 135.9, 135.6, 134.6, 129.4, 128.8, 128.5, 128.0, 127.4, 77.4, 66.1, 54.2, 40.5, 38.1, 31.9, 31.9, 29.7, 29.4, 29.3, 29.3, 29.2, 28.6, 27.1, 25.9, 22.7, 14.2 ppm. (Signals missing due to overlapping peaks.) FT-IR: ν = 3234, 3064, 2956, 2924, 2855, 1746, 1636, 1556, 1498, 1466, 1456, 1440, 1366, 1303, 1198, 1171, 739, 723, 699 cm^{-1}. MALDI-TOF-MS: calculated M = 691.49 g mol^{-1}, observed m/z = 714.41 [M + Na]$^+$, 692.38 [M + H]$^+$ g mol^{-1}. Elemental analysis: $C_{42}H_{65}N_3O_5$ (691.98). Calcd: C: 72.90, H: 9.47, N: 6.07; obs: C: 73.19, H: 9.57, N: 5.96%.

***N′*,*N″*-Dioctyl-*N*-[(*R*)-(benzyl)octyloxycarbonylmethyl]benzene-1,3,5-tricarboxamide ((*R*)-2).** BTA (*R*)-**2** was synthesized according to the procedure for the enantiomer using equal amounts of reactants. Pure BTA (*R*)-**2** was isolated as a sticky white solid (128 mg, 0.18 mmol, 60%). ^{1}H-NMR ($CDCl_3$): 8.22 (s, 1H, –ArH (core)), 8.14 (s, 2H, –ArH (core)), 7.34–7.20 (m, 5H, –Ph (Phe)), 6.63 (t, 2H, J = 5.2 Hz, –CONH–(octyl)), 5.02 (ddd, 1H, J = 7.2, 6.7, 6.0 Hz, –CONHC*H*RR′–), 4.16–4.10 (m, 2H, –$COOCH_2$–), 3.62 (d, 1H, J = 7.4 Hz, –CONH–(Phe)) 3.48–3.39 (dt, 4H, J = 5.3, 5.2 Hz, –CONHCH_2–), 3.28 (dd, 1H, J = 13.7, 6.0 Hz, Hα–CH_2Ph), 3.22 (dd, 1H, J = 13.7, 6.7 Hz, Hβ–CH_2Ph), 1.71–1.53 (m, 6H, –$COOCH_2CH_2$– + –$CONHCH_2CH_2$–), 1.44–1.19 (m, 30H, –CH_2–), 0.88 (t, 9H, J = 5.5 Hz, –CH_3) ppm. ^{13}C-NMR ($CDCl_3$) δ: 171.6, 165.6, 165.5, 135.9, 135.6, 134.6, 129.4, 128.8, 128.5, 128.0, 127.4, 77.4, 66.1, 54.2, 40.5, 38.2, 31.9, 31.9, 29.7, 29.4, 29.3, 29.3, 29.2, 28.6, 27.1, 25.9, 22.7, 14.2 ppm. (Signals missing due to overlapping

peaks.) FT-IR: $\nu = 3231, 3064, 2956, 2924, 2855, 1746, 1636, 1556, 1498, 1466, 1456, 1440, 1366, 1301, 1198, 1170, 739, 723, 699\ cm^{-1}$. MALDI-TOF-MS: calculated $M = 691.49\ g\ mol^{-1}$, observed $m/z = 714.36\ [M + Na]^+$, $692.36\ [M + H]^+\ g\ mol^{-1}$. Elemental analysis: $C_{42}H_{65}N_3O_5$ (691.98). Calcd: C: 72.90, H: 9.47, N: 6.07; obs: C: 72.65, H: 9.38, N: 5.97%.

***N*,*N*′,*N*″-Tris[(*S*)-(benzyl)octyloxycarbonylmethyl]benzene-1,3,5-tricarboxamide ((*S*,*S*,*S*)-4).** BTA (*S*,*S*,*S*)-**4** was prepared according to a literature procedure[19] using freshly prepared (*S*)-phenylalanine octyl ester and commercially available benzene-1,3,5-tricarbonyl trichloride to give the product in 70% yield. ^{1}H-NMR (DMSO-d_6) δ: 9.13 (d, 3H, $J = 7.6$ Hz, –CONH–), 8.40 (s, 3H, –ArH (core)), 7.32–7.22 (m, 12H, –Ph (Phe)), 7.22–7.16 (m, 3H, –Ph (Phe)), 4.68 (ddd, H, $J = 7.6, 6.0, 6.0$ Hz, –CONHC*H*RR′–), 4.02 (t, 6H, $J = 6.4$ Hz, –$COOCH_2$–), 3.16–3.10 (m, 6H, –CH_2Ph), 1.55–1.42 (m, 6H, –$COOCH_2CH_2$–), 1.28–1.10 (m, 30H,–CH_2–), 0.82 (t, 9H, $J = 6.7$ Hz, –CH_3) ppm. ^{13}C-NMR (DMSO-d_6) δ: 171.4, 165.4, 137.5, 134.1, 129.2, 128.9, 128.2, 126.4, 64.5, 54.5, 39.5, 36.2, 31.1, 28.5, 28.5, 28.0, 25.2, 22.0, 13.9 ppm. FT-IR: $\nu = 3231, 3063, 3030, 2954, 2926, 2856, 1742, 1638, 1558, 1497, 1456, 1363, 1325, 1197, 1168, 1109, 739, 698\ cm^{-1}$. MALDI-TOF-MS: calculated $M = 987.60\ g\ mol^{-1}$, observed $m/z = 1010.55\ [M + Na]^+$, $988.55\ [M + H]^+\ g\ mol^{-1}$. Elemental analysis: $C_{60}H_{81}N_3O_9$ (988.30). Calcd: C: 72.92, H: 8.26, N: 4.25; obs: C: 72.68, H: 8.35, N: 4.17%.

***N*,*N*′,*N*″-Tris[(*R*)-(benzyl)octyloxycarbonylmethyl]benzene-1,3,5-tricarboxamide ((*R*,*R*,*R*)-4).** BTA (*R*,*R*,*R*)-**4** was synthesized according to the procedure for the enantiomer using equal amounts of reactants. Pure BTA (*R*,*R*,*R*)-**4** was obtained as a sticky white solid (1.80 g, 83%). ^{1}H-NMR (DMSO-d_6) δ: 9.13 (d, 3H, $J = 7.7$ Hz, –CONH–), 8.40 (s, 3H, –ArH (core)), 7.32–7.22 (m, 12H, –Ph (Phe)), 7.22–7.14 (m, 3H, –Ph (Phe)), 4.68 (ddd, H, $J = 7.6, 6.0, 6.0$ Hz, –CONHC*H*RR′–), 4.02 (t, 6H, $J = 6.4$ Hz, –$COOCH_2$–), 3.19–3.08 (m, 6H, –CH_2Ph), 1.55–1.42 (m, 6H, –$COOCH_2CH_2$–), 1.30–1.11 (m, 30H, –CH_2–), 0.82 (t, 9H, $J = 6.8$ Hz, –CH_3) ppm. ^{13}C-NMR (DMSO-d_6) δ: 171.4, 165.4, 137.5, 134.1, 129.2, 128.9, 128.2, 126.4, 64.5, 54.5, 36.2, 31.1, 28.5, 28.5, 27.9, 25.2, 22.0, 13.9 ppm. FT-IR: $\nu = 3231, 3063, 3030, 2954, 2926, 2856, 1742, 1639, 1558, 1497, 1456, 1364, 1326, 1197, 1168, 1109, 739, 699\ cm^{-1}$. MALDI-TOF-MS: calculated $M = 987.60\ g\ mol^{-1}$, observed $m/z = 1010.49\ [M + Na]^+$, $988.49\ [M + H]^+\ g\ mol^{-1}$. Elemental analysis: $C_{60}H_{81}N_3O_9$ (988.30). Calcd: C: 72.92, H: 8.26, N: 4.25; obs: C: 72.74, H: 8.19, N: 4.05%.

Acknowledgements

M.V. and A.P. thank Council for the Chemical Sciences of the Netherlands Organization for Scientific Research (CW-NWO) for financial support.

References and notes

1 M. Kristiansen, P. Smith, H. Chanzy, C. Baerlocher, V. Gramlich, L. McCuskcr, T. Weber, P. Pattison, M. Blomenhofer and H. W. Schmidt, *Cryst. Growth Des.*, 2009, **9**, 2556–2558.
2 J. Roosma, T. Mes, P. Leclère, A. R. A. Palmans and E. W. Meijer, *J. Am. Chem. Soc.*, 2008, **130**, 1120–1121.
3 C. F. C. Fitié, I. Tomatsu, D. Byelov, W. H. de Jeu and R. P. Sijbesma, *Chem. Mater.*, 2008, **20**, 2394–2404.
4 K. Hanabusa, C. Koto, M. Kimura, H. Shirai and A. Kakehi, *Chem. Lett.*, 1997, 429–430.
5 D. Ogata, T. Shikata and K. Hanabusa, *J. Phys. Chem. B*, 2004, **108**, 15503–15510.
6 M. P. Lightfoot, F. S. Mair, R. G. Pritchard and J. E. Warren, *Chem. Commun.*, 1999, 1945–1946.
7 J. J. van Gorp, J. A. J. M. Vekemans and E. W. Meijer, *J. Am. Chem. Soc.*, 2002, **124**, 14759–14769.
8 L. Brunsveld, A. P. H. J. Schenning, M. A. C. Broeren, H. M. Janssen, J. A. J. M. Vekemans and E. W. Meijer, *Chem. Lett.*, 2000, 292–293.
9 M. M. J. Smulders, I. A. W. Filot, J. M. A. Leenders, P. van der Schoot, A. R. A. Palmans, A. P. H. J. Schenning and E. W. Meijer, *J. Am. Chem. Soc.*, 2010, **132**, 611–619.
10 M. M. J. Smulders, P. J. M. Stals, T. Mes, T. F. E. Paffen, A. P. H. J. Schenning, A. R. A. Palmans and E. W. Meijer, *J. Am. Chem. Soc.*, 2010, **132**, 620–626.
11 T. F. A. de Greef, M. M. J. Smulders, M. Wolffs, A. P. H. J. Schenning, R. P. Sijbesma and E. W. Meijer, *Chem. Rev.*, 2009, **109**, 5687–5754.
12 P. J. M. Stals, J. C. Everts, R. de Bruijn, I. A. W. Filot, M. M. J. Smulders, R. Martin-Rapun, E. A. Pidko, T. E. A. de Greef, A. R. A. Palmans and E. W. Meijer, *Chem.–Eur. J.*, 2010, **16**, 810–821.
13 P. J. M. Stals, M. M. J. Smulders, R. Martín-Rapún, A. R. A. Palmans and E. W. Meijer, *Chem.–Eur. J.*, 2009, **15**, 2071–2080.
14 M. M. J. Smulders, A. P. H. J. Schenning and E. W. Meijer, *J. Am. Chem. Soc.*, 2008, **130**, 606–611.
15 K. P. van den Hout, R. Martín-Rapún, J. A. J. M. Vekemans and E. W. Meijer, *Chem.–Eur. J.*, 2007, **13**, 8111–8123.
16 A. R. A. Palmans, J. A. J. M. Vekemans, E. E. Havinga and E. W. Meijer, *Angew. Chem., Int. Ed. Engl.*, 1997, **36**, 2648–2651.
17 I. A. W. Filot, E. A. Pidko, A. R. A. Palmans, E. W. Meijer, R. A. van Santen and T. F. A. de Greef, *J. Phys. Chem. B.*, 2010, DOI: 10.1021/jp1072928.
18 P. P. Bose, M. G. B. Drew, A. K. Das and A. Banerjee, *Chem. Commun.*, 2006, 3196–3198.
19 M. de Loos, J. H. van Esch, R. M. Kellogg and B. L. Feringa, *Tetrahedron*, 2007, **63**, 7285–7301.
20 M. M. Green, J. W. Park, T. Sato, A. Teramoto, S. Lifson, R. L. B. Selinger and J. V. Selinger, *Angew. Chem., Int. Ed.*, 1999, **38**, 3139–3154.
21 J. van Gestel, A. R. A. Palmans, B. Titulaer, J. A. J. M. Vekemans and E. W. Meijer, *J. Am. Chem. Soc.*, 2005, **127**, 5490–5494.
22 M. Kasha, H. R. Rawls and M. A. El-Bayoumi, *Pure Appl. Chem.*, 1965, **11**, 371–392.
23 M. M. J. Smulders, M. M. L. Nieuwenhuizen, T. F. A. De Greef, P. van der Schoot, A. P. H. J. Schenning and E. W. Meijer, *Chemistry*, 2010, **16**, 362–367.
24 M. M. J. Smulders, I. A. W. Filot, J. M. A. Leenders, P. van der Schoot, A. R. A. Palmans, A. P. H. J. Schenning and E. W. Meijer, *J. Am. Chem. Soc.*, 2009, **132**, 611–619.
25 M. M. J. Smulders, P. J. M. Stals, T. Mes, T. F. E. Paffen, A. P. H. J. Schenning, A. R. A. Palmans and E. W. Meijer, *J. Am. Chem. Soc.*, 2009, **132**, 620–626.
26 J. van Gestel, P. van der Schoot and M. A. J. Michels, *Macromolecules*, 2003, **36**, 6668–6673.
27 To exclude slow kinetics upon mixing, a solution with 58% ee was annealed for 3 h at 90 °C and cooled again to 20 °C. No differences in the magnitude or shape of the CD effect were observed before and after annealing of the solution.
28 Depending on the wavelength at which the CD effect is monitored, the shape of the titration curves can vary. This is a direct result of the different shape of the CD spectra.
29 Annealing of a sample containing 55% (*S*,*S*,*S*)-**4** for 2 h at 90 °C did not show any difference in either the size or shape of the observed CD-spectra compared to the non-annealed sample, thereby showing the instantaneous spectral changes upon mixing.
30 The exact structure of the 1 : 1 heterocomplex formed between (*S*,*S*,*S*)-**4** and $(octyl)_3$ BTA is unknown.